

Effect of Electron Beam Irradiation on Structural, Electrical and Thermo-electric Power of $\text{La}_{0.8}\text{Sr}_{0.2}\text{MnO}_3$

Ashok Rao^{1,*}, J. Benedict Christopher¹, Ganesh Sanjeev², G.S. Okram³

¹ Department of Physics, Manipal Institute of Technology, Manipal University, Manipal-576104, India

² Microtron Centre, Mangalore University, Mangalagangothri – 574199, DK, Karnataka, India

³ UGC-DAE Consortium for Scientific Research, University Campus, Indore-452017, India

(Received 05 December 2014; published online 25 March 2015)

In this communication, we are reporting the effect of electron beam (e-beam) irradiation on thermoelectric properties of $\text{La}_{0.8}\text{Sr}_{0.2}\text{MnO}_3$ manganites. The samples were prepared using solid state reaction technique. It is observed that the lattice volume increases with increase in dosage of e-beam. With irradiation an increase in resistivity is observed. For small irradiation dosage, we first observe a decrease in metal-insulator transition temperature T_{MI} ; thereafter T_{MI} increases with further increase in dosage of irradiation. Both, the resistivity data and thermo-electric power data demonstrate that small polaron hopping model is valid in high temperature region.

Keywords: Solid state reaction technique, Electrical resistivity, Thermoelectric power.

PACS numbers: 81.20.Ev, 72.15.Eb, 72.15.Jf

1. INTRODUCTION

Ever since the discovery of colossal magneto-resistance effect (CMR) and large magneto-caloric effect in rare earth manganite of the form $\text{RE}_{1-x}\text{A}_x\text{MnO}_3$ (RE is a rare-earth element, A is a divalent alkaline element), immense work has been done on the electrical, magnetic and thermal properties of these materials [1-9]. The primary aim of such studies is to understand the physics behind these properties and to explore possibilities of using them in various applications [10]. These manganites show numerous interesting properties like metal-insulator transition, and paramagnetic-ferromagnetic transition. Over the decades, energetic ion-beams and electron beams have been used as a vital tool for modification of materials [11, 12]. Extensive work seems to have been done on various ion irradiations. Chattopadhyay et al. [13] have shown that La^{3+} ion irradiation creates disorder in $\text{La}_{0.7}\text{Ca}_{0.3}\text{MnO}_3$ (LCMO) manganite sample and as a result of this an increase in room temperature resistivity is observed. Ravi Kumar et al. [14] has reported the influence of swift heavy ion irradiation on transport properties of thin films of LCMO system and have demonstrated that T_C decreases with increase in fluence of the beam. On the other hand they have reported that the resistivity of the films increases with fluence value. Kataria et al. [15] have reported interesting results which indicate that thickness of films of LPMO plays important role and they have demonstrated that for small thickness of 150 nm, irradiated films have lower resistivity than pristine films of same thickness. However, for films of thickness 150 nm and above, an increase in resistivity is seen when the samples are irradiated. $\text{La}_{1-x}\text{Sr}_x\text{MnO}_3$ (LSMO) in particular has attracted lot of attention as they are considered to be prototypical and reference materials [16, 17]. They are promising materials since they show ferromagnetic-paramagnetic transition and also exhibit significant magneto-resistance (MR) value

[18, 19] which essentially make them promising candidates for applications. Sahasrabudhe et al. [20] have done a detailed investigation on the effect of heavy ion irradiation on the surface morphology of highly oriented thin films of LSMO and concluded using XRD that irradiation induces strain in the films. Less work seems to have been done on effect of electron beam irradiation on manganites. Samoilenko et al. [21] have demonstrated that when thin films of LSMO are irradiated by KrF laser emitting in the UV range, the metallic phase of the film is observed to increase. Pallecchi et al. [22] have investigated the effect of focused ion beam (Ga ion) on LSMO films and have shown that resistivity increases with increases in dosage of irradiation.

To the best of our knowledge, no work seems to have been done electron beam irradiation on LSMO system. Keeping this in mind, we have investigated the effect of electron beam irradiation on structural, electrical and thermo-electric properties of $\text{La}_{0.8}\text{Sr}_{0.2}\text{MnO}_3$ compounds. We have focused the present studies on thermoelectric power as it is sensitive to the nature of charge carriers. The Seebeck coefficient (S) of manganites exhibits a complex behavior indicating both positive and negative signs which depends on temperature as well as on the nature and degree of substitution. In the low temperature regime S is related to the changes in electronic structure and scattering processes, whereas in the insulating region S provides information on energy dependent parameters which follow small polaron hopping mechanism. Thus it would be interesting to see the effect of electron beam irradiation on thermoelectric power of $\text{La}_{0.8}\text{Sr}_{0.2}\text{MnO}_3$ compounds.

2. EXPERIMENTAL

In this work, single phase polycrystalline strontium-substituted lanthanum manganite ($\text{La}_{0.8}\text{Sr}_{0.2}\text{MnO}_3$) compounds were prepared by conventional solid state reaction technique. Stoichiometric amounts of lantha-

* ashokanu_rao@rediffmail.com

num oxide (La_2O_3), strontium carbonate (SrCO_3), and manganese oxide (MnO_2) were weighed and mixed thoroughly. The finely ground stoichiometric mixture of the starting materials was calcined in air several times at 1200°C for 24 hours with a final calcination at 1250°C for 24 hours. The obtained powder after calcination was uni-axially pressed into pellets (rectangular pellets of thickness ≈ 1.5 mm) by applying pressure ≈ 80 kg/cm². Finally the samples were sintered at 1350°C for 24 hours. All the samples were cooled to room temperature at a cooling rate of about $3^\circ\text{C}/\text{min}$.

In order to ascertain the purity and to determine the lattice dimensions, X-ray diffraction (XRD) technique was used (D8 Advanced X-ray Diffractometer). The data taken from XRD was analyzed using Rietveld refinement method. Then the samples were irradiated by electron beam irradiation. It may be mentioned that all the samples were prepared under identical conditions. We have carried out electron beam irradiation using an 8 MeV electron accelerator which is able to provide energetic electrons, intense bremsstrahlung radiation and neutrons of moderate flux. The accelerator provides pulsed electron beam current of 50 mA (peak) with a pulse width of ~ 2.5 μs at a maximum pulse repetition rate of 100 Hz. Electrical resistivity measurements on the rectangular shaped samples were carried out in a temperature range of 10-380 K in a cryostat (Closed Cycle Refrigerator by JANIS). The resistivity of the samples was measured using conventional four probe technique employing a Keithley current source and a Keithley nano-voltmeter. The Seebeck coefficient measurement was performed in the temperature range of 5-340 K using differential dc method in a closed cycle refrigerator.

3. RESULTS AND DISCUSSION

Fig. 1 shows the room temperature X-ray diffraction patterns of bulk samples of $\text{La}_{0.8}\text{Sr}_{0.2}\text{MnO}_3$ at different dosage levels of electron beam in the range of 0-50 kGy. The diffraction data was refined using Rietveld refinement technique and Rietveld refined plots are shown in the Fig. 2. The open circles show the actual data, the calculated curve is superimposed on them, the solid line represents the refined data and the vertical lines represent the Bragg peak. We observe that there is good agreement between the observed and refinement data which confirms that the prepared samples are free from secondary or impurity phase. From the refinement procedure we observe that the samples are rhombohedral in structure with R3c space group and the structure does not change with irradiation. The lattice parameters and structure estimated in the present work match well with that reported in literature [23].

We now discuss the effect of electron beam irradiation on structural properties. From table 1 it is evident that both a and c parameters increase with dosage level of electron beam thereby volume increases with EB dosage. It is also seen that there is an increase in Mn-O-Mn bond length which may be attributed to introduction of magnetic inhomogeneity due to EB irradiation [24].

The temperature dependence of the resistivity (ρ) for the samples of $\text{La}_{0.8}\text{Sr}_{0.2}\text{MnO}_3$ over a temperature

range, 100-380 K is illustrated in Fig. 3. It is evident from the ρ - T plot, that all the samples undergo metal to insulator transition (MI) around the characteristic temperature T_{MI} . For the pristine sample the value of T_{MI} is about 314 K. For the sample irradiated with dosage of 15 kGy, a decrease in T_{MI} is observed. However, with further increase in electron beam dosage, T_{MI} increases with dosage. It is evidently from Fig. 3 that there is continuous suppression in peak resistivity with increase dosage of electron irradiation. The observed drop in resistivity with electron beam irradiation may be attributed to relaxation of strain in the lattice via irradiation. This is consistent with the observed increase in cell volume of the lattice. Similar results have been reported by Chattopadhyay et al. [25] for ion beam

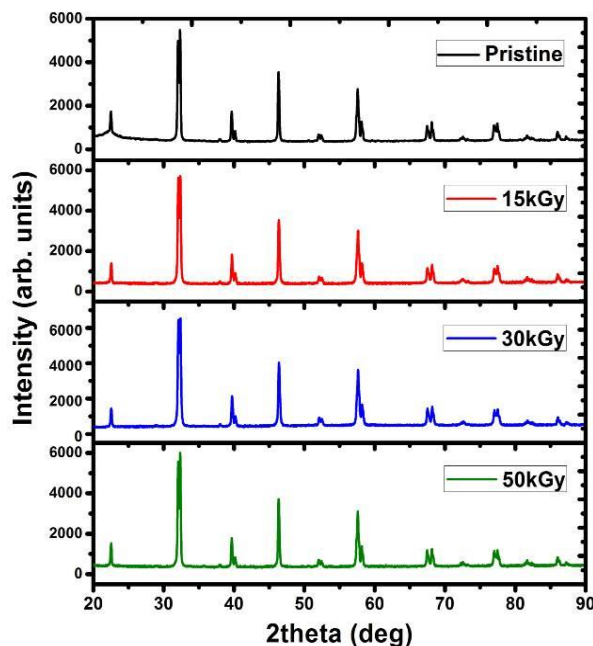


Fig. 1 – XRD patterns of pristine as well as electron beam irradiated samples of $\text{La}_{0.8}\text{Sr}_{0.2}\text{MnO}_3$

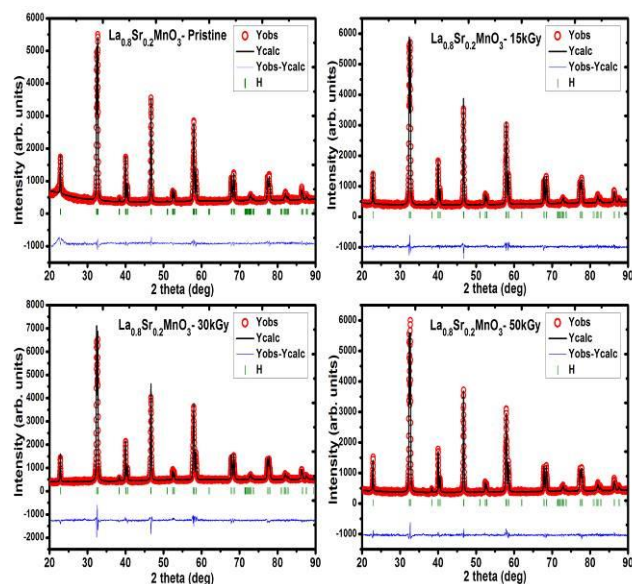


Fig. 2 – Rietveld refined XRD plots for the pristine and irradiated samples $\text{La}_{0.8}\text{Sr}_{0.2}\text{MnO}_3$

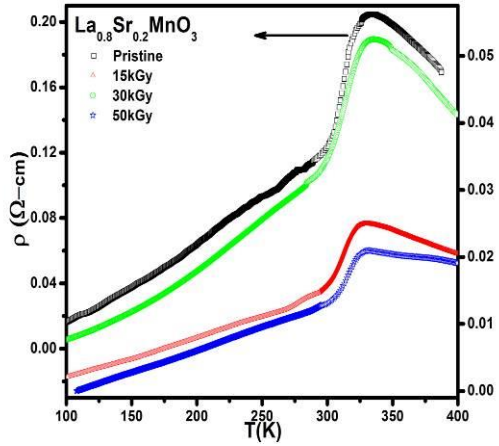


Fig. 3 – Resistivity versus temperature behavior of pristine as well as electron beam irradiated samples of $\text{La}_{0.8}\text{Sr}_{0.2}\text{MnO}_3$

irradiated samples of $\text{Li}_{0.7}\text{Pb}_{0.3}\text{MnO}_3$ which has been attributed to radiation induced strain relaxation and ordering in the lattice.

In order to understand the conduction phenomenon at low temperatures, the electrical resistivity in the low temperature region (ferromagnetic metallic phase) below T_{MI} is fitted using the equation,

$$\rho(T) = \rho_0 + \rho_2 T^2 + \rho_{4.5} T^{4.5} \quad (1)$$

where ρ_0 is the residual resistivity due to grain boundary scattering, ρ_2 is arising from electron-electron scattering (e^-e^-), and $\rho_{4.5}$ is the resistivity factor due to various effects of e^-e^- , e^- -magnon and e^- -phonon scattering processes. In the present work we have used the experimental data of resistivity and have fitted it using Eq. 1. It is satisfactory to note that the experimental data matches well with the above equation. The fitting parameters are presented in Table 1. We observe that $\rho_0 \gg \rho_2$ and $\rho_0 \gg \rho_{4.5}$ which indicates that the electron-electron scattering is the dominating factor for the conduction phenomenon in the low temperature region.

Table 1 – Best fit parameters for low temperature region

Dosage	ρ_0	ρ_2	$\rho_{4.5}$
0	9.6×10^{-3}	1.7×10^{-6}	-2.4×10^{-13}
15	9.1×10^{-3}	1.7×10^{-7}	-6.6×10^{-15}
30	3.6×10^{-3}	3.8×10^{-7}	-2.6×10^{-14}
50	2.1×10^{-3}	2.2×10^{-7}	-3.7×10^{-14}

We also observe that ρ_0 decreases with dosage of electron beam. This implies that electron beam irradiation is reducing the electron-electron scattering which would mean that there should be reduction in resistivity of the samples when they are irradiated with electron beam. This indeed is observed which is evident from Fig. 3.

We now analyze the high temperature resistivity data using small polaron hopping (SPH) using the equation,

$$\rho(T) = \rho_0 T \exp(E_p / k_B T) \quad (2)$$

We have used the high temperature resistivity data (above T_{MI}) and fitted the data using Eq. 2. It is satis-

factory to note that the present results in the high temperature regime follow SPH model. Using this model we have estimated activation energy E_p for the pristine as well as irradiated samples of $\text{La}_{0.8}\text{Sr}_{0.2}\text{MnO}_3$. The estimated parameters are tabulated in Table 2.

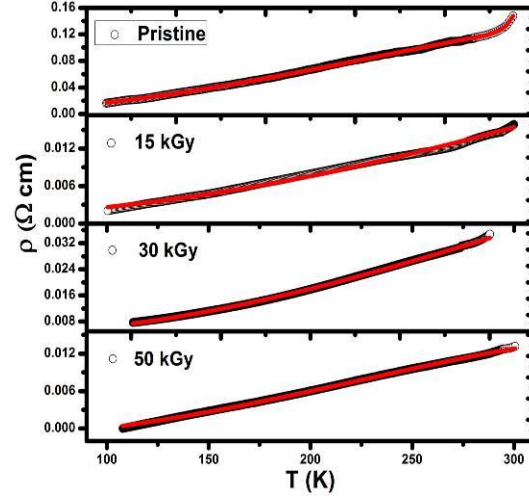


Fig. 4 – Fitting of low temperature resistivity data of pristine and irradiated samples of $\text{La}_{0.8}\text{Sr}_{0.2}\text{MnO}_3$

Table 2 – Best fit parameters for high temperature region

Dosage	E_p (meV)
0	73.3
15	75.7
30	80.3
50	90.3

Fig. 5 depicts the high temperature resistivity data along with the fitted curves for pristine and irradiated samples. We notice two features. Firstly the experimental data match well with the theoretical fitting. Secondly the estimated value of activation energy is observed to increase in dosage of electron beam.

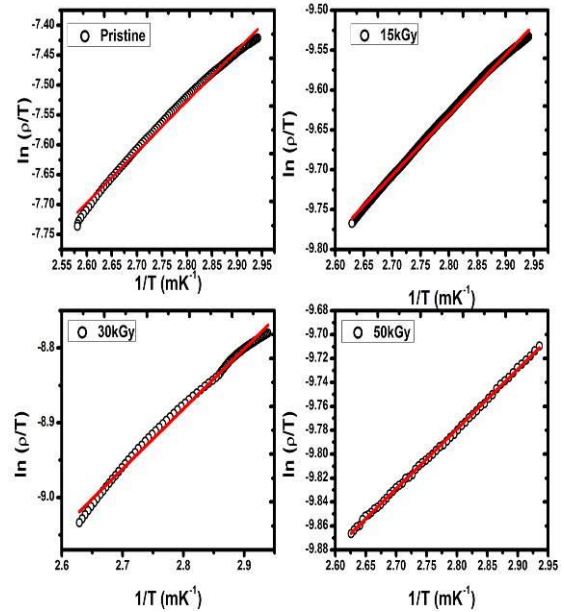


Fig. 5 – Fitting of high temperature resistivity data of pristine and irradiated samples of $\text{La}_{0.8}\text{Sr}_{0.2}\text{MnO}_3$

In view to elucidate other evident features of the pristine as well as irradiated samples, Seebeck coefficient (S) was measured in the temperature range of 5-340 K. The plots of the measurement are presented in Fig. 6.

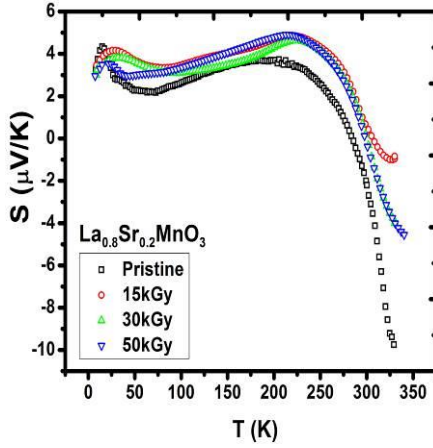


Fig. 6 – Thermo-electric power versus temperature behavior of pristine as well as electron beam irradiated samples of $\text{La}_{0.8}\text{Sr}_{0.2}\text{MnO}_3$

We observe that for the pristine sample, $S(T)$ is negative for high temperature region. As the temperature is reduced we observe a change in sign of $S(T)$. This negative to positive crossover indicates that the nature of charge carriers is changing from electron to holes as the samples are becoming more conducting with electron beam irradiation. This is consistent with electrical resistivity data. We further see that $S(T)$ decreases with reduction in temperature. At a particular temperature, a peak value in $S(T)$ is observed. Thereafter, with further decrease in temperature $S(T)$ is seen to decrease. The negative $S(T)$ at the high temperature regime is due to electrons which are excited into the conduction band from the valence band. This trend is seen in pristine as well as irradiated samples.

Akin to the electrical resistivity, many scattering mechanisms are responsible for the total $S(T)$ in different temperature ranges. Hence we analyze the contribution of different scattering mechanisms to the temperature dependent $S(T)$ data in the metallic and insulating regimes. First we analyze the thermo-electric power data in the metallic region. For this region we have utilized the following well-known equation,

$$S(T) = S_0 + S_{3/2}T^{3/2} + S_4T^4 \quad (3)$$

where S_0 is a constant, $S_{3/2}T^{3/2}$ arises due to electron-magnon scattering and S_4T^4 arises due to spin wave fluctuations in the FM region. We observe that the thermo-electric power data in metallic region matches well with Eq. 3. Fig. 7 shows the experimental $S(T)$ data with theoretical values and demonstrates a good match between the two. The fitting parameters are presented in Table 3. The value of $S_{3/2}$ is observed to be much larger compared to S_4 thereby demonstrating that the e-magnon scattering process is dominant mechanism in the low temperature metallic region.

For the present studies, $S(T)$ data in the insulating regime is analyzed within the framework of small polaron hopping model [35]. Figure 8 shows a plot of S

versus $1/T$ and it is satisfactory to see that the present data fits well with SPH model.

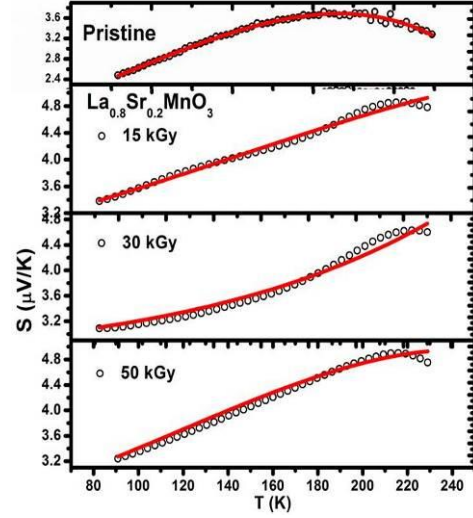


Fig. 7 – Fitting of $S(T)$ in the metallic region for the pristine and irradiated samples of $\text{La}_{0.8}\text{Sr}_{0.2}\text{MnO}_3$

Table 1 – Best fit parameters for low temperature region

Dosage	S_0	$S_{3/2}T^{3/2}$	S_4T^4
0	1.25	1.5×10^{-3}	1.1×10^{-9}
15	2.72	7.7×10^{-4}	1.8×10^{-10}
30	2.67	3.8×10^{-4}	3.0×10^{-10}
50	2.22	1.2×10^{-4}	4.7×10^{-10}

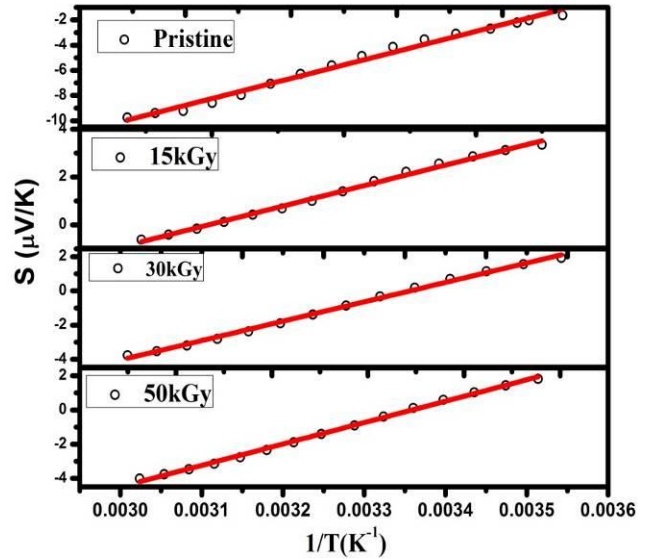


Fig. 8 – Fitting of $S(T)$ in the insulating for the pristine and irradiated samples of $\text{La}_{0.8}\text{Sr}_{0.2}\text{MnO}_3$

4. SUMMARY

The structural, electrical and thermo-electric properties of pristine and irradiated samples of $\text{La}_{0.8}\text{Sr}_{0.2}\text{MnO}_3$ are reported in this communication. We observe that there is no change in structure of the sample upon electron beam irradiation. However, it is seen that the volume of the lattice increases with increase in dosage of irradiation which means that irradiation induces strain in the lattice. The electrical resistivity measurements demon-

strate that there is a decrease in resistivity with increase in dosage of electron beam irradiation. This means that irradiation enhances conductivity of the manganites. Thermo-power measurements along with the resistivity measurements demonstrate that small polaron hopping model is valid in the high temperature insulating region

REFERENCES

1. J.B. Goodenough, *Phys. Rev.* **100**, 564 (1955).
2. J.H. Kuo, H.U. Anderson, D.M. Sparlin, *J. Solid State Chem.* **87**, 55 (1990).
3. H. Kamata, Y. Yonemura, J. Mizusaki, H. Tagawa, K. Naraya, T. Sasamoto, *J. Phys. Chem. Solids* **56**, 943 (1995).
4. Y. Tokura, *Rep. Prog. Phys.* **69**, 797 (2006).
5. M. Hervieu, A. Barnabé, C. Martin, A. Maignan, B. Raveau, *Phys. Rev. B* **60**, R726 (1999).
6. M. Pekała, V. Drozd, *J. Alloy. Compd.* **456**, 30 (2008).
7. S. Gupta, R. Ranjit, C. Mitra, P. Raychaudhuri, R. Pinto, *Appl. Phys. Lett.* **78**, 362 (2001).
8. K.P. Shinde, S.S. Pawar, N.G. Deshpande, J.M. Kim, Y.P. Lee, S.H. Pawar, *Mater. Chem. Phys.* **129**, 180 (2011).
9. A. Gaur, G.D. Varma, *J. Phys. Condens. Matt.* **18**, 8837 (2006).
10. V.S.R. Channu, *New J. Glas. Ceram.* **03**, 29 (2013).
11. T. Zhang, Z. Song, M. Sun, B. Liu, S. Feng, B. Chen, *Appl. Phys. A* **90**, 451 (2007).
12. A. Meldrum, L.A. Boatner, R.C. Ewing, *J. Mater. Res.* **12**, 1816 (1997).
13. S. Chattopadhyay, R. Kumar, A. Sarkar, *Nucl. Instrum. Meth. Phys. Res. Sect. B* **244**, 132 (2006).
14. R. Kumar, S.K. Arora, D. Kanjilal, G.K. Mehta, R. Bathe, S.K. Date, S.R. Shinde, L.V. Saraf, S.B. Ogale, S.I. Patil, *Radiat. Eff. Defects Solids* **147**, 187 (1999).
15. B. Kataria, P.S. Solanki, U. Khachar, M. Vagadia, A. Ravalia, M.J. Keshvani, P. Trivedi, D. Venkateshwarlu, V. Ganesan, K. Asokan, N.A. Shah, D.G. Kuberkar, *Radiat. Phys. Chem.* **85**, 173 (2013).
16. M.P. Gutiérrez, J. Mira, J. Rivas, *Phys. Lett. A* **323**, 473 (2004).
17. P. Jha, T.D. Sands, L. Cassels, P. Jackson, T. Favaloro, B. Kirk, J. Zide, X. Xu, A. Shakouri, *J. Appl. Phys.* **112**, 063714 (2012).
18. A. Asamitsu, Y. Moritomo, R. Kumai, Y. Tomioka, Y. Tokura, *Phys. Rev. B* **54**, 1716 (1996).
19. S. Gupta, R. Ranjit, C. Mitra, P. Raychaudhuri, R. Pinto, *Appl. Phys. Lett.* **78**, 362 (2001).
20. M.S. Sahasrabudhe, D.N. Bankar, A.G. Banpurkar, S.I. Patil, K.P. Adhi, R. Kumar, *Nucl. Instrum. Meth. Phys. Res. Sect. B* **263**, 407 (2007).
21. Z.A. Samoilenko, V.D. Okunev, E.I. Pushenko, T.A. D'yachenko, A. Cherenkov, P. Gierlowski, S.J. Lewandowski, A. Abal'oshev, A. Klimov, A. Szewczyk, *Tech. Phys.* **48**, 250 (2003).
22. I. Pallecchi, L. Pellegrino, E. Bellingeri, A.S. Siri, D. Marré, G.C. Gazzadi, *J. Magn. Magn. Mater.* **320**, 1945 (2008).
23. D. Grossin, J.G. Noudem, *Solid State Sci.* **6**, 939 (2004).
24. Z.-W. Wu, J. Li, S.-L. Li, D.-N. Zheng, *Chinese Phys. B* **22**, 087503 (2013).
25. S. Chattopadhyay, A. Sarkar, A. Banerjee, S. Karmakar, D. Banerjee, R. Kumar, B.K. Chaudhuri, *Nucl. Instrum. Meth. Phys. Res. Sect. B* **226**, 274 (2004).

ACKNOWLEDGEMENTS

The authors are thankful to Department of Atomic Energy, Board of Research in Nuclear Sciences (DAE-BRNS), Government of India, for financially supporting this work (2011/34/22/BRNS).